


 Cite this: *Chem. Commun.*, 2022, 58, 13147

 Received 9th September 2022,
 Accepted 26th October 2022

DOI: 10.1039/d2cc04990b

rsc.li/chemcomm

First observation of $[\text{Pu}_6(\text{OH})_4\text{O}_4]^{12+}$ cluster during the hydrolytic formation of PuO_2 nanoparticles using H/D kinetic isotope effect†

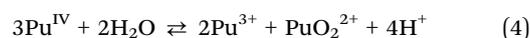
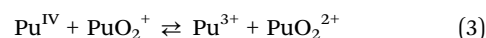
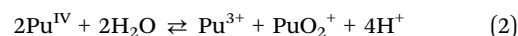
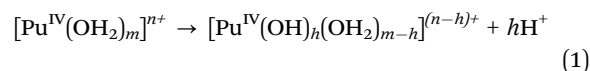
 Manon Cot-Auriol,^a Matthieu Viro, ^{*a} Thomas Dumas, ^b Olivier Diat, ^a Denis Menut, ^c Philippe Moisy, ^b and Sergey I. Nikitenko ^a

New insights are provided about the formation mechanism of PuO_2 nanoparticles (NPs) by investigating an unprecedented kinetic isotope effect observed during their hydrolytic synthesis in H_2O or D_2O and attributed to OH/OD zero point energy difference. The signature of a Pu(IV) oxo-hydroxo hexanuclear cluster, appearing as an important intermediate during the formation of the 2 nm PuO_2 NPs (synchrotron SAXS/XAS), is further revealed indicating that their formation is controlled by H-transfer reactions occurring during hydroxo to oxo-bridge conversions.

Anthropogenic activities significantly contribute to the release of plutonium in the environment and related colloids are currently interrogated about their role in the migration of radioactivity in aquatic systems.^{1–4} Pu chemistry in aqueous solution involves complex processes including redox/disproportionation, hydrolysis and complexation reactions that can particularly compete for the (+IV) redox state.^{5,6} Pu(IV) is indeed highly prone to hydrolysis and the subsequent formation of oligomers that further condensate yielding intrinsic colloids and/or precipitates, even under acidic conditions.^{7–9} Meanwhile, disproportionation of Pu(IV) and Pu(V) significantly contribute to the accumulation of ionic Pu(VI), Pu(V) and Pu(III) species during their formation.^{7,8,10} While recent investigations reach a consensus in describing intrinsic Pu colloids as *ca.* 2 nm PuO_2 -like NPs, much less is known about their formation mechanism.^{11–14} The description of Pu oxo-hydroxo clusters, with a characteristic size situated somewhere between the ones of ionic and colloidal species of Pu, highlighted the relation between their core structures revealing some striking similarities with bulk PuO_2 . This suggested that bigger clusters could

be formed from the assembly of those smaller molecular fragments.^{5,15–18} A better knowledge about the underlying mechanism would help in understanding the behaviour of these species in environmental context and pave the way for pioneering approaches devoted to the control of the size-property relationship of Pu nanomaterials.¹³ Kinetic isotope effect (KIE) can be observed when comparing reaction rates in H_2O and D_2O .¹⁹ Primary KIE originates from the cleavage of O–H bonds and differs from solvent isotope effect which is related to differences in the physico-chemical properties of H_2O and D_2O solvents (pK_w , polarity, viscosity...²⁰ In this work, H/D KIE was explored to probe the formation mechanism of colloidal PuO_2 NPs.

The formation kinetics of intrinsic Pu(IV) colloids was monitored by Vis-NIR absorption spectroscopy (Fig. 1) by diluting a Pu(IV) concentrated solution in H_2O or D_2O (ESI†). It is important to mention that the pH (pD) of the studied solutions is imposed by the acidity of the added Pu(IV) solution aliquot (the slight pK_w difference resulting from self-ionization of H_2O and D_2O is not responsible for KIE described below, ESI†). After a few minutes in H_2O , the characteristic electronic signature from Pu(IV) colloids (resulting from Pu(IV) hydrolysis, eqn (1)) was observed with a main absorption band located around 616 nm and several others at 578, 688 and 735 nm (Fig. 1a).²¹ The sharp absorption band at 830 nm was attributed to the additional presence of Pu(VI) in solution (PuO_2^{2+} form, less than *ca.* 3% of total Pu) resulting from Pu(IV) disproportionation (eqn (2)–(4)).^{9,22}



Pu(III) concentration should be *ca.* twice the one of Pu(VI) according to eqn (2)–(4) but it is hardly observed due to low

^a ICSM, Univ Montpellier, CEA, CNRS, ENSCM, Marcoule, France.

E-mail: matthieu.viro@cea.fr

^b CEA, DES, ISEC, DMRC, Univ Montpellier, Marcoule, France

^c Synchrotron SOLEIL, L'Orme des Merisiers, Départementale 128, 91190 Saint Aubin, France

 † Electronic supplementary information (ESI) available: Additional spectra, experimental details and methods. See DOI: <https://doi.org/10.1039/d2cc04990b>

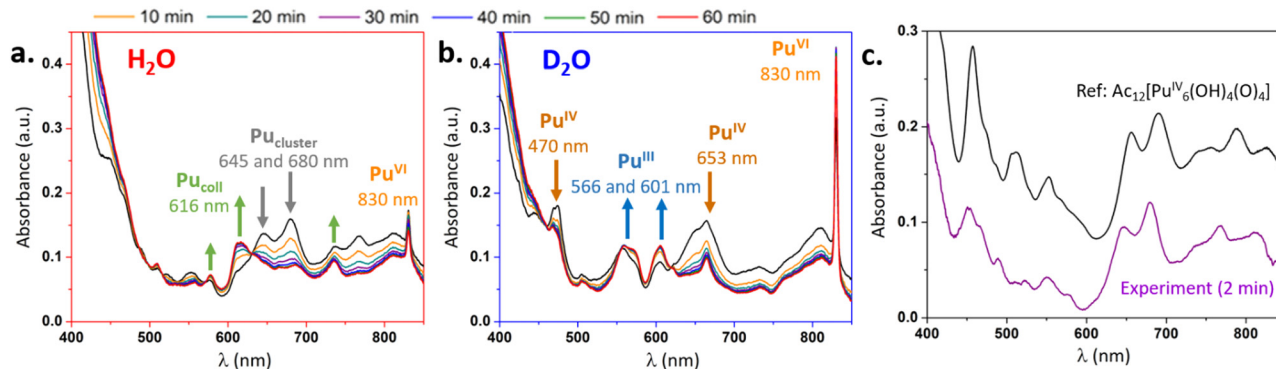



Fig. 1 Vis-NIR absorption spectra acquired during the synthesis of Pu(IV) colloids in (a) H₂O and (b) D₂O in the 2–60 min range. (c) Vis-NIR absorption spectrum acquired 2 min after dispersion of concentrated Pu(IV) in H₂O (without contributions of Pu(III), Pu(VI) and Pu_{colloid}) compared to Pu(IV) acetate hexanuclear cluster, with courtesy of C. Tamain.¹⁵

molar coefficient ($33 \text{ M}^{-1} \text{ cm}^{-1}$) and the superposition of the various transitions in the 600–700 nm spectral range. The absorption spectra acquired in D₂O for similar other conditions evolved differently. In particular, indisputable signatures of Pu(IV) (hydrolyzed forms, 470 nm and 653 nm) and Pu(III) (Pu³⁺ form at 601 nm and 566 nm) were observed contrasting with experiments carried out in H₂O.^{9,22} Also, the determined amount of Pu(VI) at 830 nm was much higher in D₂O (*ca.* 15% of total Pu) (Fig. 1b). After several weeks and despite strong kinetic differences, both aged H₂O and D₂O solutions of Pu converged to stable Pu(IV) intrinsic colloids as evidenced by characteristic absorption spectra (Fig. S3, ESI†). Such a behaviour is attributed to KIE occurring during Pu(IV) hydrolysis and leading to slowdown of Pu colloid formation.^{23,24}

A closer look at the electronic spectra acquired during the first hour in H₂O medium (Fig. 1a) allows observing an original transient species with principal absorption bands located at 680 and 645 nm. The spectrum appears directly after Pu(IV) dilution in H₂O (spectra at 2 min) and decreases in absorbance with time while the characteristic spectra of the Pu colloids appear. An isobestic point observed at 630 nm suggests a two-component conversion. Deconvolution studies which consisted in the subtraction of reference spectra (Pu(III–VI) and Pu_{colloid}) from the experimental ones revealed an unprecedented signature (Fig. 1c) which offered striking similarities with a recently described oxo-hydroxo hexanuclear core of a Pu(IV) cluster [Pu₆(OH)₄O₄]¹²⁺ decorated by acetate or DOTA ligands.^{15,16} Slight differences between both spectra were attributed to the decoration of the latter with acetate ligands (on-going efforts aim at stabilizing this species during Pu(IV) colloid synthesis). A similar observation in D₂O appeared more complicated due to the important contribution of other Pu ionic species originated from Pu(IV) disproportionation and hydrolysis. The deconvoluted spectrum revealed a noisy signal most likely attributed to low concentrated Pu(IV) polynuclear cores including the hexamer or Pu(IV) hydrolysed species (Fig. S4, ESI†).

Kinetic curves were extracted from deconvolution studies (approach described in ESI†) to understand the observed reactivity differences during the first minutes. Fig. 2a and b

confirm the more important disproportionation of Pu(IV) (with a stronger accumulation of ionic Pu(VI) and Pu(III) in solution) and the lower concentration of the Pu cluster intermediate in D₂O medium. Pu(VI) concentration is twice the one of Pu(III) in agreement with the eqn (4). Note that Pu(V) was not observed during deconvolution but its presence in the process can't be excluded. In both media, Pu(VI) quickly accumulated in solution during *ca.* 30 min before slowly decreasing with time (Fig. 2c). The initial accumulation rate of Pu(VI) was found to be slightly higher in D₂O than in H₂O ($20.1 \text{ vs. } 5.2 \text{ mM h}^{-1}$, respectively).

After *ca.* 30 min, Pu(VI) consumption was explained by its reaction with Pu(III) (*i.e.* Pu(IV) comproportionation). A first order reaction law was used on Pu(VI) to compare both kinetics in agreement with the work of Rabideau and Kline (eqn (S2), ESI†).²⁵ It is interesting to note that the logarithm function only fitted in the 30–120 min range for H₂O medium which was attributed to the evolution of Pu species during comproportionation and a possible alternative mechanism when Pu(VI) and Pu(III) show a very low concentration in solution.⁹ Fig. 2c evidences the significantly higher reduction rate of Pu(VI) observed in H₂O ($k^{\text{H}}(-\text{Pu}^{\text{VI}})/k^{\text{D}}(-\text{Pu}^{\text{VI}}) = 6.8$). The consumption of Pu(III) was not considered due to its low absorbance and the interferences with the spectra of other Pu species. Deconvolutions also allowed to estimate the formation kinetics of Pu(IV) colloids at *ca.* 616 nm (Fig. 2d). Assuming a first order formation rate on the colloid (eqn (S5), ESI†), it was confirmed that the latter accumulates at a much lower rate in D₂O. The calculated ratio of the colloid formation kinetic constants $k^{\text{H}}(\text{Pu}_{\text{colloid}})/k^{\text{D}}(\text{Pu}_{\text{colloid}})$ equalled 7.4.

Synchrotron measurements allowed the quasi-simultaneous characterization of the aged (>1 month) colloids by small-angle X-ray scattering (SAXS) and X-ray absorption spectroscopy (XAS) without altering the nature of the samples (Fig. S5, ESI†). Normalized SAXS diagrams exhibited similar scattering profiles in both cases (Fig. S6, ESI†), characteristic from sharp interfaces typical for 3D dense particles.²⁶ Considering a simple model of spherical and homogeneous NPs with a slight polydispersity (0.15), the data adjustment provided a slightly higher radius for the colloid formed in D₂O ($1.1 \pm 0.1 \text{ nm}$ *vs.*



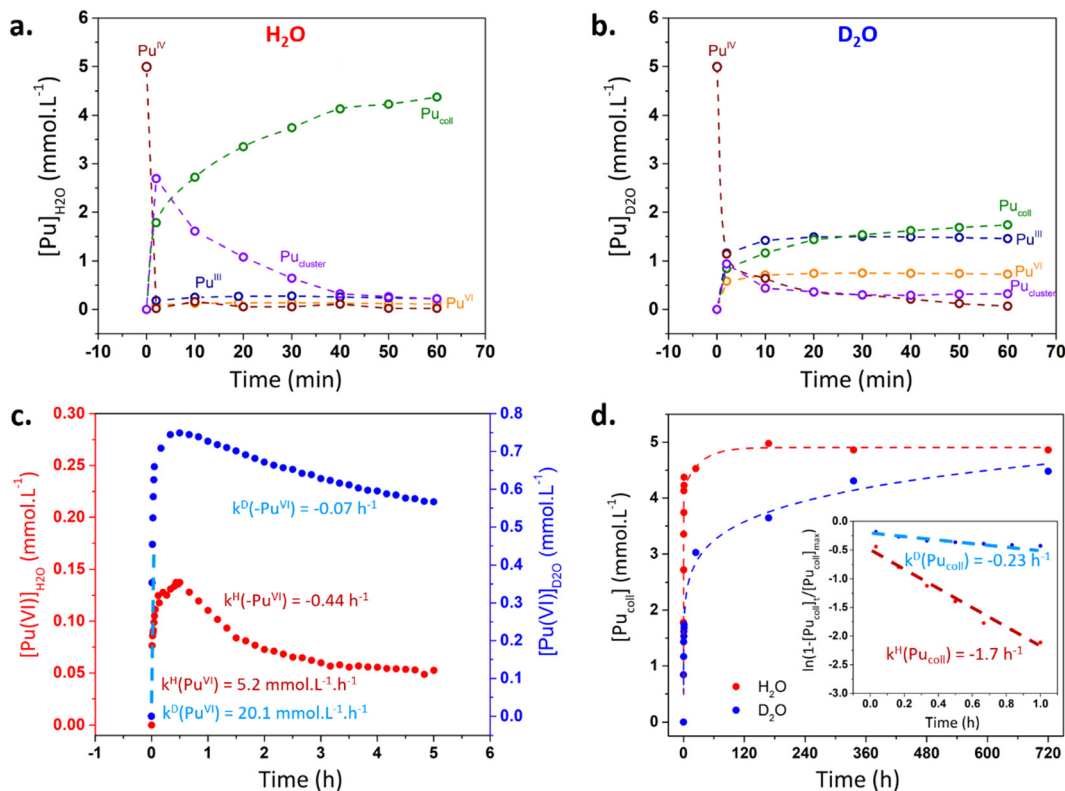


Fig. 2 (a and b) Kinetics related to Pu species in H₂O and D₂O after deconvolution. (c) Evolution of Pu(vi) concentration during the synthesis of Pu(iv) colloids in H₂O and D₂O. A special care should be given to scale bar differences. Dashed lines represent linear regressions used to determine kinetic rates (corresponding values given in ESI†). (d) Evolution of the colloid absorbance ($\lambda = 616$ nm) as a function of time after deconvolution of the absorbance spectra. Insert: plot of the natural logarithm of Pu colloid absorbance against time.

0.9 ± 0.1 nm in H₂O). The determined scattering length density (ca. 69 10¹⁰ cm⁻²) and the volume fraction were very close to the estimated parameters (Table S3, ESI†). This simple model, with few but consistent parameters, is well representative of the scattering signal variation in absolute scale.

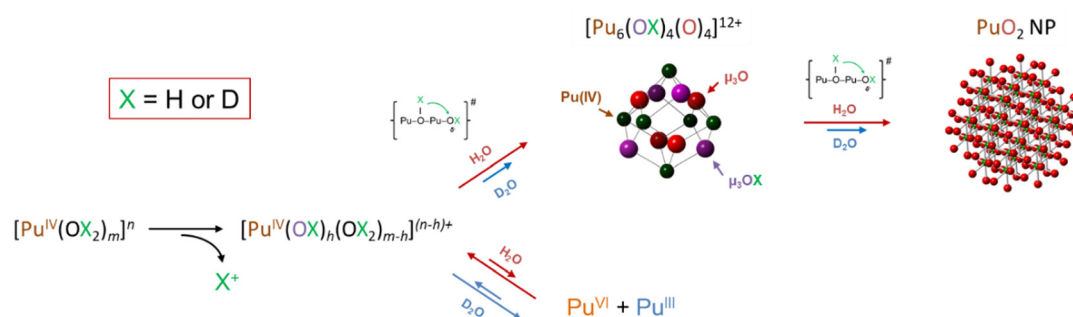
X-ray absorption near-edge structure (XANES) spectra acquired at the Pu L₃ edge on the colloids formed in both media exhibited a white line (18067 eV) at similar positions, agreeing with the strong predominance of the (+IV) oxidation state for Pu (Fig. S7, ESI†).^{27,28} A slight difference observed on the spectra at ca. 18080 eV was attributed to the significant contribution of Pu(vi) ions in D₂O. In order to compare the data obtained in H₂O and D₂O, a XAS spectrum of Pu(vi) was subtracted from the experimental data obtained in D₂O (Fig. S8, ESI†).^{27,28} The resulting EXAFS spectrum was found to be similar to the one acquired in H₂O (Fig. S7, ESI†). Both FT showed two main peaks at $R-\varphi =$ ca. 1.84 and 3.68 Å, agreeing with Pu(iv) colloids^{11,26,29} and crystalline bulk PuO₂ (CFC, *Fm*3̄m).^{7,30} The structural parameters of the fits demonstrated that local structures of the colloids prepared in this study are similar and close to bulk PuO₂ (Table S5, ESI†).

As a first conclusion, the observed strong KIE only shows little influence on the final shape, size and local structure of the NPs which can be described as 2 nm spherical NPs with a PuO₂-like local structure.^{7,11,14,26,31,32} The physico-chemical property

differences reported for H₂O and D₂O at room temperature and originating solvent isotope effects in some cases cannot explain the observed KIE.²⁰ As well, it has been demonstrated that quantum tunnelling observed for electron or H atom transfer is more important in H₂O than in D₂O.³³ Such a phenomenon could have been invoked to explain a faster disproportionation of Pu(iv) in H₂O which is not the case in our study (Fig. 2c). By contrast, the KIE can be explained by the zero point energy difference between O–H and O–D bonds ($\Delta E = 5.89$ kJ mol⁻¹).^{19,34} As a consequence, more energy is required to break the latter bonds favouring disproportionation of Pu(iv) in D₂O medium instead of the cluster formation. Therefore, O–H bond ruptures appear as rate-limiting steps during the colloid formation. The calculated theoretical isotopic separation factor $\alpha_{(H/D)}$ equals 10.6 at $T = 300$ K (eqn (S6), ESI†) which is in good agreement with the k^H/k^D ratios observed for Pu(vi) reduction and Pu colloid formation. Interestingly, kinetic studies related to hydrolysis in D₂O are scarce in the literature. We only found one recent publication describing the hydrolysis of Ce(iv) and subsequent formation of CeO₂ NPs with a close ratio $k^H/k^D = 10$.³⁵

It has been argued that Pu(iv) disproportionation is preceded by Pu(iv) ion hydrolyses and the generation of polynuclear hydroxo complexes.³⁶ The slightly higher accumulation rates observed for Pu(vi) in D₂O after disproportionation suggest that hydrolysis of Pu(iv) (eqn (1)) is poorly affected by KIE. By contrast,





Scheme 1 Scheme of the formation mechanism of the colloidal PuO₂ nanoparticles.

both the cluster core and Pu colloid formation are limited in D₂O. The presence of hydroxo-bridges in the hexanuclear cluster and their absence in the final oxo-NP demonstrates that the Pu colloid formation involves a succession of olation and oxolation reactions confirming that PuO₂ NPs formation is limited by H-atom transfer reactions (Scheme 1).^{6,18} This observation further discards classical crystal nucleation theory for PuO₂ NPs in aqueous media where crystal growth occurs through the addition of monomeric units³⁷ but rather suggests the stacking of metastable and structurally well-defined oxo-hydroxo Pu(IV) clusters as a favoured mechanism,¹⁷ as also suggested for U(IV) cluster analogues.^{38,39}

We acknowledge RCHIM/RTA project (cross-cutting basic research program) for its financial support. This study was also partially supported by grants from the CNRS Interdisciplinary Project “Nucléaire, Energie, Environnement, Déchets, Société (NEEDS)”.

Conflicts of interest

There are no conflicts to declare.

References

- G. J.-P. Deblonde, A. B. Kersting and M. Zavarin, *Commun. Chem.*, 2020, **3**, 167.
- A. Yu. Romanchuk, I. E. Vlasova and S. N. Kalmykov, *Front. Chem.*, 2020, **8**, 630.
- A. B. Kersting, *Inorg. Chem.*, 2013, **52**, 3533–3546.
- E. L. Tran, O. Klein-BenDavid, N. Teutsch and N. Weisbrod, *Environ. Sci. Technol.*, 2015, **49**, 13275–13282.
- L. Soderholm, P. M. Almond, S. Skanthakumar, R. E. Wilson and P. C. Burns, *Angew. Chem., Int. Ed.*, 2008, **47**, 298–302.
- D. A. Costanzo, R. E. Biggers and J. T. Bell, *J. Inorg. Nucl. Chem.*, 1973, **35**, 609–622.
- J. Rothe, C. Walther, M. A. Denecke and Th Fanghänel, *Inorg. Chem.*, 2004, **43**, 4708–4718.
- V. Neck and J. I. Kim, *Radiochim. Acta*, 2001, **89**, 1–16.
- D. L. Clark, S. S. Hecker, G. D. Jarvinen and M. P. Neu, *The chemistry of the actinide and transactinide elements*, Springer, Netherland, Dordrecht, 2006, pp. 813–1264.
- C. Walther, H. R. Cho, C. M. Marquardt, V. Neck, A. Seibert, J. I. Yun and T. Fanghänel, *Radiochim. Acta*, 2007, **95**, 7–16.
- E. Dalodière, M. Viro, V. Morosini, T. Chave, T. Dumas, C. Hennig, T. Wiss, O. Dieste Blanco, D. K. Shuh, T. Tyliszczak, L. Venault, P. Moisy and S. I. Nikitenko, *Sci. Rep.*, 2017, **7**, 43514.
- M. Viro, T. Dumas, M. Cot-Auriol, P. Moisy and S. I. Nikitenko, *Nanoscale Adv.*, 2022, DOI: [10.1039/D2NA00306F](https://doi.org/10.1039/D2NA00306F).
- E. Gerber, A. Yu Romanchuk, S. Weiss, A. Kuzenkova, M. O. J. Y. Hunault, S. Bauters, A. Egorov, S. M. Butorin, S. N. Kalmykov and K. O. Kvashnina, *Environ. Sci.: Nano*, 2022, **9**, 1509–1518.
- E. Gerber, A. Yu Romanchuk, I. Pidchenko, L. Amidani, A. Rossberg, C. Hennig, G. B. M. Vaughan, A. Trigub, T. Egorova, S. Bauters, T. Plakhova, M. O. J. Y. Hunault, S. Weiss, S. M. Butorin, A. C. Scheinost, S. N. Kalmykov and K. O. Kvashnina, *Nanoscale*, 2020, **12**, 18039–18048.
- D. Chupin, C. Tamain, T. Dumas, P. L. Solari, P. Moisy and D. Guillaumont, *Inorg. Chem.*, 2022, **61**, 4806–4817.
- C. Tamain, T. Dumas, D. Guillaumont, C. Hennig and P. Guilbaud, *Eur. J. Inorg. Chem.*, 2016, 3536–3540.
- K. E. Knope and L. Soderholm, *Inorg. Chem.*, 2013, **52**, 6770–6772.
- G. E. Sigmon and A. E. Hixon, *Chem. – Eur. J.*, 2019, **25**, 2463–2466.
- S. Scheiner and M. Čuma, *J. Am. Chem. Soc.*, 1996, **118**, 1511–1521.
- G. Swain and F. W. Bader, *Tetrahedron*, 1960, **10**, 182–199.
- M. H. Lloyd and R. G. Haire, *Radiochim. Acta*, 1978, **25**, 139–148.
- D. Jebaraj Mahildoss and T. N. Ravi, *J. Radioanal. Nucl. Chem.*, 2012, **294**, 87–91.
- S. W. Rabideau, *J. Am. Chem. Soc.*, 1953, **75**, 798–801.
- S. W. Rabideau and R. J. Kline, *J. Phys. Chem.*, 1960, **64**, 680–682.
- S. W. Rabideau and R. J. Kline, *J. Phys. Chem.*, 1958, **62**, 617–620.
- C. Micheau, M. Viro, S. Dourdain, T. Dumas, D. Menut, P. L. Solari, L. Venault, O. Diat, P. Moisy and S. I. Nikitenko, *Environ. Sci.: Nano*, 2020, **7**, 2252–2266.
- T. Vitova, I. Pidchenko, D. Fellhauer, T. Pruessmann, S. Bahl, K. Dardenne, T. Yokosawa, B. Schimmelpfennig, M. Altmaier, M. Denecke, J. Rothe and H. Geckeis, *Chem. Commun.*, 2018, **54**, 12824–12827.
- S. D. Conradson, D. L. Clark, M. P. Neu, W. Runde and C. D. Tait, *Los Alamos Sci.*, 2000, **26**, 418–421.
- C. Ekberg, K. Larsson, G. Skarnemark, A. Ödegaard-Jensen and I. Persson, *Dalton Trans.*, 2013, **42**, 2035–2040.
- A. Kuzmin and J. Chaboy, *IUCr*, 2014, **1**, 571–589.
- M. Altmaier, X. Gaona and D. Fellhauer, in *Plutonium Handbook*, ed. D. A. Geeson, D. L. Clark and R. J. Hanrahan Jr., American Nuclear Society, La Grange Park, IL, USA, 2019, vol. 3.
- L. Bonato, M. Viro, T. Dumas, A. Mesbah, E. Dalodière, O. Dieste Blanco, T. Wiss, X. Le Goff, M. Odorico, D. Prieur, A. Rossberg, L. Venault, N. Dacheux, P. Moisy and S. I. Nikitenko, *Nanoscale Adv.*, 2020, **2**, 214–224.
- T. Kumagai, M. Kaizu, S. Hatta, H. Okuyama, T. Aruga, I. Hamada and Y. Morikawa, *Phys. Rev. Lett.*, 2008, **100**, 166101.
- M. Ceriotti, W. Fang, P. G. Kusalik, R. H. McKenzie, A. Michaelides, M. A. Morales and T. E. Markland, *Chem. Rev.*, 2016, **116**, 7529–7550.
- N. W. Pettinger, R. E. A. Williams, J. Chen and B. Kohler, *Phys. Chem. Chem. Phys.*, 2017, **19**, 3523–3531.
- J. M. Haschke, *J. Nucl. Mater.*, 2007, **362**, 60–74.
- J. De Yoreo, *Nat. Mater.*, 2013, **12**, 284–285.
- L. Chatelain, R. Faizova, F. Fadaei-Tirani, J. Pécaut and M. Mazzanti, *Angew. Chem., Int. Ed.*, 2019, **58**, 3021–3026.
- N. P. Martin, C. Volklinger, N. Henry, X. Trivelli, G. Stoclet, A. Ikeda-Ohno and T. Loiseau, *Chem. Sci.*, 2018, **9**, 5021–5032.

